



HAL
open science

Design of magnetorheological brake for forearm rotation of a wrist prosthesis

Rina Dutra, Fernanda Ferreira, Guilherme Rubio, Joao Pereira, Rafael de
Andrade, Claysson Vimieiro

► **To cite this version:**

Rina Dutra, Fernanda Ferreira, Guilherme Rubio, Joao Pereira, Rafael de Andrade, et al.. Design of magnetorheological brake for forearm rotation of a wrist prosthesis. ICORR 2022 - 17th International Conference on Rehabilitation Robotics, Jul 2022, Rotterdam, Netherlands. pp.1-6, 10.1109/ICORR55369.2022.9896503 . hal-03828249

HAL Id: hal-03828249

<https://inria.hal.science/hal-03828249>

Submitted on 27 Dec 2022

HAL is a multi-disciplinary open access archive for the deposit and dissemination of scientific research documents, whether they are published or not. The documents may come from teaching and research institutions in France or abroad, or from public or private research centers.

L'archive ouverte pluridisciplinaire **HAL**, est destinée au dépôt et à la diffusion de documents scientifiques de niveau recherche, publiés ou non, émanant des établissements d'enseignement et de recherche français ou étrangers, des laboratoires publics ou privés.

Design of magnetorheological brake for forearm rotation of a wrist prosthesis*

Rina M. A. Dutra^{1,2}, Fernanda M. R. M. Ferreira², Guilherme P. Rúbio², João V. F. M. Pereira³,
Rafael M. de Andrade⁴, and Claysson B. S. Vimieiro^{2,5}

Abstract— A wrist joint in upper limb prostheses significantly increases its handling capacity. However, current prostheses cannot reproduce the ability of torque combined with the volume and weight of the human wrist. Consequently, they do not provide high efficiency in handling and generate user dissatisfaction. In this context, this study aims to optimal design a wrist supination and pronation brake to improve the handling capacity of an upper limb prosthesis. The wrist actuator consists of an EC motor and harmonic drive parallel with a magnetorheological brake. The brake guarantees a fast response time, low energy consumption, controllability, and small dimensions. A particle swarm algorithm is applied to optimize design variables to minimize mass and energy consumption. As a result, the brake provided resistive torque of 7.4 N.m with dimensions close to a healthy member and weighing 0.1972 kg. Finally, a finite element analysis confirmed a satisfactory magnetic flux for the magnetorheological brake operating conditions. The designed brake addressed all the desired characteristics and is suitable to integrate the forearm prosthesis with wrist rotation.

Index terms— Prosthetic Wrist, Pronation/Supination, MR Brake, Optimal Design.

I. INTRODUCTION

Pronation and supination movements are essential for an amputee's daily living activities [1]. The condition of the rehabilitation results is associated with analyzing the strength of pronation and supination of the forearm [2]. Although, the pronation and supination movement has been relatively little discussed in the generation of wrist torque in prosthesis [1]. From a mechanical point of view, current actuators require a larger space than is appropriate to represent rotational

movement with the same intensity as the human body [3]. Besides that, Wrist prostheses with pronation/supination movement tend to be passive, activated by body movement, and when active, present as a method of actuation of DC motors or ultrasonic motors [4]. These motors have a high torque and energy consumption ratio and promote heat dissipation [5].

Prosthetic wrists do not have an ideal pronation/supination mechanism [4], compromising the ability to reproduce the human wrist in terms of torque, strength, and compactness. Consequently, they limit the manipulation of resources and the quality of life of amputees [6]. The challenge is to design prosthetic wrists that accurately control joint torque while allowing users to be free and comfortable to perform functional tasks, keeping the wrist at different angles and different arm postures without compromising workspace and execution speed [7, 8].

One way to achieve this result is to use magnetorheological (MR) fluid, which has replaced conventional dry friction brakes and hydraulic brakes in prosthetic systems [9]. Brakes with MR fluid, or MR brakes, are devices that can reduce the angular velocity of a rotary axis immersed in the MR fluid [10]. Unlike hydraulic systems, the resistance offered by the MR fluid is activated instantly and only when the individual needs it [9]. MR brakes are very effective in maintaining the position of the joints against external forces, where the rotational stiffness of the joint can vary in real-time as the amputee needs it [5, 9]. In addition, they can maintain high output torque with less current and less heat dissipation than an electric motor [5]. Thus, fluid control ensures a range of motion, level of damping, and strength according to the activity performed by the amputee, contributing to the design of a reliable and intelligent prosthesis [11]. As it is a fluid-filled brake, it does not make mechanical noise and, in addition, allows the development of devices with smaller sizes, higher dynamic ranges, low failure rate, and high regulation capacity [12, 13].

The use of MR fluid in prosthesis design provides the user with greater comfort and reproduction of moving closer to the natural movement and with less energy consumption [14, 15]. In this context, this work aims to design a magnetorheological brake for the pronation and supination movement of a prosthetic wrist. Compared to existing wrist design approaches, it is expected to obtain a system with more adequate characteristics to reproduce the move, considering the resistive torque capacity, shape, weight, and energy consumption of the MR fluid. Although no studies are using the MR fluid in prosthetic wrists, studies that applied the MR fluid in joints similar to the wrist in haptics devices [16-18] and rehabilitation devices via telemedicine [19] confirmed

* This research was partially funded by grants from FAPES (Fundação de Amparo à Pesquisa e Inovação do Espírito Santo, TO 151/2021 Project No. 2021-8GJZ6 and TO 460/2021 Project No. 2021-L7SZ4) and MCTI/FINEP (Financiadora de Estudos e Projetos, public company linked to the Ministério da Ciência, Tecnologia e Inovações, Project 21.01.0101.00, Ref. 2790/20).

¹R. M. A. Dutra is with the Centre for Innovation, Research and Teaching in Mechatronics (NIPEM), Universidade Federal de São João del-Rei, Ouro Branco, MG 36420-000 Brazil (corresponding author to provide e-mail: rina@ufsj.edu.br).

²R. M. A. Dutra, F. M. R. M. Ferreira, G. P. Rúbio and C. B. S. Vimieiro are with Postgraduate Program in Mechanical Engineering, Universidade Federal de Minas Gerais, Belo Horizonte, MG 31270-901 Brazil.

³J. V. F. M. Pereira is with Department of Mechanical Engineer, Universidade Federal de Minas Gerais, Belo Horizonte, MG 31270-901 Brazil.

⁴R. M. de Andrade is with Department of Mechanical Engineer, Universidade Federal do Espírito Santo, Vitória, ES 29075-910 Brazil.

⁵C. B. S. Vimieiro is with the Graduate Program in Mechanical Engineering, Pontifícia Universidade Católica de Minas Gerais, Belo Horizonte, MG 30.535-901 Brazil.

these results. In addition, the proposed wrist may have other applications since the development of prosthetic devices that represent the wrist joint can be used in other areas, such as in medical service robots and industrial manipulators [3].

II. WORKING PRINCIPLE

Pronation/supination can be seen as the movement of the forearm or wrist in which the forearm rotates around its longitudinal axis [1, 20]. The concentration of rotation on the wrist facilitates the development of mechanisms in the prosthesis without losing functionality and movement biomechanics. An average human forearm weighs about 1.1 kg (excluding the hand), has a length of about 26 cm, and can be surrounded by a trunk cone with a larger base radius of 4.5 cm and a smaller base radius of 3 cm [7]. The pronation and supination movement of the forearm has an amplitude of 180° [4]. However, a 100° rotation (50° pronation and 50° supination) is sufficient to perform most activities of daily living, such as opening a door, using the telephone, reading a newspaper, drinking, or eating something [21].

The torque intensity of the pronation and supination movements for activities of daily living and work is well below the maximum values achieved by a forearm. Ciriello, et al. [22] indicated that basic activities such as clockwise screwing of the right hand have a maximum isometric torque of 6.76 N.m. If performed for 15 min or 25 min, the proper torque is 1.46 N.m and 1.15 N.m, respectively. In industrial workers, the maximum acceptable torques to avoid discomfort and ergonomic problems vary from 1.15 N.m and 1.88 N.m in pronation/supination activities, such as screwing [23]. Lorenz, et al. [24] showed that during orthopedic procedures, surgeons are subject to pronation/supination torques of 1.76 N.m in repetitive efforts. For activities of daily living, such as eating soup or eating vegetables, the maximum torque does not reach 1 N.m [25].

Regarding the angular velocity of the pronation and supination movement, Kaneko, et al. [26] performed a test with 40 volunteers. The authors found that the highest mean velocities were 73.5 rpm in pronation with the elbow in the 180° position and 73.3 rpm in supination with the elbow in the 135° position. However, in basic activities such as transferring a cup or a place block, the maximum speed during the pronation and supination movement was approximately 50 rpm [27].

A prosthetic wrist must present a torque of at least 7 N.m, with an approximate angular velocity of up to 50 rpm, and weigh a maximum of 1.1 kg, to reproduce the movement of the human wrist in activities of daily living. With these restrictions, an EC motor (EC 45 Flat, Maxon Motors, Switzerland) (70 W and 141 g) and a gearbox (CSG-14-100-2A-RE, Harmonic Drive AG, Germany) (reduction ratio of 100:1 and 90 g) were selected to guarantee the requirements and at the same time provide a compact system. This assembly offers 8.4 N.m of maximum torque and 47.5 rpm of angular speed.

The proposed MR brake was designed to parallel this motor-reducer system. This configuration ensures sufficient resistive torque for the wrist pronation/supination movement with fast response time, high torque/weight ratio, high

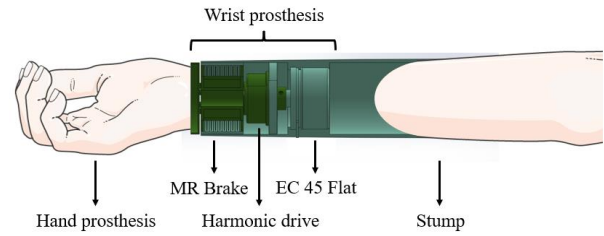


Figure 1. Cutaway view of the wrist prosthesis. The light green color represents the structure connected to the stator and the dark green color represents the structure connected to the rotor.

torque/volume, and easy controllability. Brakes are one of the most commercially used magneto-rheological fluid devices and are generally composed of rotor, stator, coil, and MR fluid [10]. The stator (light green) is designed to be connected to the amputee's residual limb (stump). In contrast, the rotor (dark green) is connected to the hand prosthesis, with relative movement between the stator and rotor, as shown in Fig. 1.

The operating principle is based on using a small amount of magneto-rheological fluid located in the clearance between the brake rotor and stator [19]. As the fluid shear tension increases, the friction force applied to the rotor will increase, resulting in a resistive torque on the brake output shaft [19]. Therefore, the resistive torque is obtained by passing an electric current through the magnetic core [17]. Consequently, the MR brake can reduce or stop the rotational speed of a shaft using the MR effect, which is generated between the rotor and the stator [28]. Furthermore, this proposed configuration can provide a sufficient resistive torque (90% of the maximum torque) in 80 ms, a fast time compared to other prosthetic devices [29].

Torque transmissibility in the MR brake occurs in shear mode, commonly used in prostheses because it provides small forces [10]. The fluid is sheared parallel to the rotating disk relative to the other disk, with a magnetic field applied perpendicular to the direction of movement of these shear surfaces [30], according to Fig. 2. The multidisc

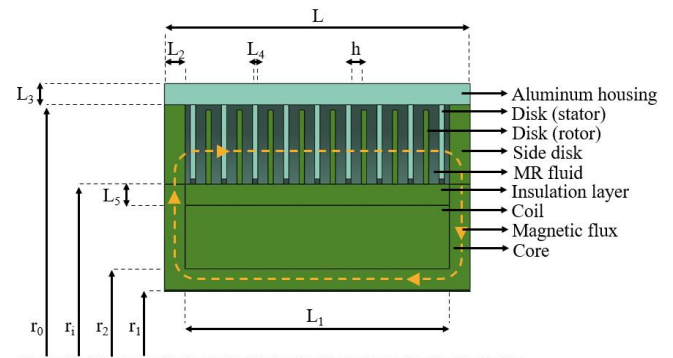


Figure 2. Configuration of the MR brake. L is the width of the MR brake, L_1 is the width of the coil, L_2 is the thickness of the thickness of the side disks, L_3 is the aluminium cover thickness, L_4 is the thickness of the input/output disks, L_5 is the thickness of the insulation layer of the thickness of the coil, h is the working gap thickness, r_1 is the iron core, r_2 is the lower inner radius of the iron core, r_1 is the inner radius of the disks and r_0 is the outer radius of the disks. The light green color represents the structure connected to the stator and the dark green color represents the structure connected to the rotor.

configuration provided better torque density in prosthetic devices [29, 31, 32].

The functioning of the prosthesis occurs actively when only the motor is working and resistively when only the magneto-rheological brake operates. The movement will be free when both are in the off state. An example of the operating mode for the activity of eating soup is shown in Fig. 3. In this case, it considered the initial movement with the forearm resting on the table (event 1), the user taking the cutlery and taking it to the plate (event 2), taking a certain amount of soup to his mouth (event 3), returning with his forearm to the table (event 4) and staying with the forearm on the table (event 5). For events 1 and 5, where there is no need for the presence of torque control, to have movement, it is necessary to overcome the inertia of the motor-reducer system (MR brake off and EC 45 Flat off). For events 2 to 4, a control strategy can be developed to ensure energy savings and movement stability, establishing the best moments for active, semi-active, or passive movement. For example, in event 3, when the user has a quantity of food in the spoon, the action can only be passive (MR brake on and EC 45 Flat off). If it is necessary to reproduce an active movement (MR brake off and EC 45 Flat off) due to, for example, the need to tilt the spoon, the control strategy can activate the motor-reducer system. The system also provides a fourth mode of operation, functioning as a semiactive prosthesis, when, for example, the system's battery is low.

These operation modes can be applied to any activity of daily living, as they contemplate any torque phase during a pronation and supination movement. Machine learning as a control strategy will be proposed in future work. Activity classification can be done through a previous database or in a real control interactively. Such functioning increases the device's potential as a prosthetic application since the pronation and supination movement do not have a standard curve torque and may require resistive torque for a long time and in different periods depending on the activity performed. It will determine the best operating mode and, consequently, improve energy consumption and system stability.

III. OPTIMAL DESIGN OF MR BRAKE

A. Dimensioning of the Magnetorheological Brake

For prosthetic applications, the fluid shear rate is small. So, the Bingham model can predict the rheological behavior

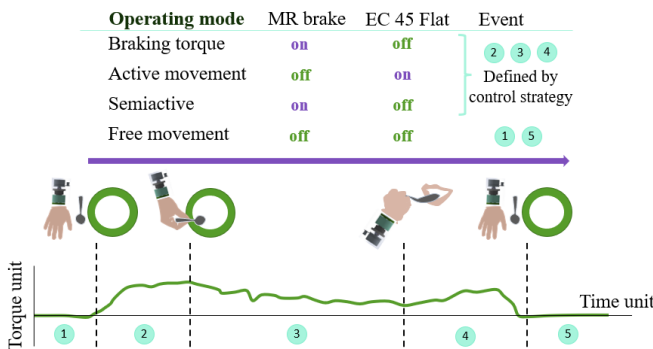


Figure 3. Operating modes of the system (MR brake + EC 45 Flat / Harmonic drive) during the soup activity.

of the fluid [23]. Bingham plastic materials act as a rigid body at low stresses and behave like a viscous fluid at high stresses [12]. The output torque of the MR brake is calculated through the fluid flow stress interaction with half the total area of the disks as only half of the disks are sheared by the fluid, while the other half is connected to the stator. The resistive output torque (T) of the multidisc configuration is defined by (1) [33]. N is the total number of gaps, τ_y is the fluid shear limit stress that varies as a function of the applied external magnetic field, r_o is the outer radius, r_i is the inner radius, ω is the angular velocity of the disks, μ_{MR} is the dynamic viscosity of the MR fluid and h is the height of the gaps.

$$T = 2N\pi[\tau_y/3(r_o^3 - r_i^3) + \omega\mu_{MR}/4h(r_o^4 - r_i^4)] \quad (1)$$

The first term in the equation (more to the left) is the torque induced by the magnetic field. The second term represents the off-state torque, which is the only term present in the absence of a magnetic field. Once the torque is defined, the coil must provide a sufficient magnetic flux density to reach the desired yield strength for the correct functioning of the brake. Therefore, it is necessary to evaluate the magnetic intensity applied to the MR fluid gap. As shown by Andrade, et al. [33], the flux of the magnetic field (φ) defined by (2) is a function of the number of turns in the coil (N_b), current (I), width (l_i), magnetic permeability (μ_i), and cross-sectional area (A_i), where i represents the infinitesimal component of the magnetic circuit.

$$\varphi = N_b I / \sum(l_i / \mu_i A_i) \quad (2)$$

The denominator of (2) represents the equivalent reluctance of the magnetic circuit. The equation variables and the magnetic flux of the MR brake are geometrically represented in Fig. 2.

B. MR Brake Optimization

The objective of ideal design is to find significant geometric dimensions of MRF-based devices that minimize an objective function considering typical characteristics such as resistive torque, mass, and energy consumption [30]. In this way, a Particle Swarm Optimization (PSO) algorithm was implemented to promote the optimization of the MR brake. The PSO is a computational method commonly used in prosthetic design with MRF that optimizes a problem by iteratively improving a candidate solution with low operating cost and a fast convergence rate [9, 33]. The objective function (OBJ) was defined for the mass and energy consumption of the MR brake (3). Reducing these parameters is relevant to permitting heavy components' installation, longer battery life, and providing a lightweight prosthetic device [33-35]. Therefore, a weight factor (α) of 70% was adopted for mass (M) and a weight factor (β) of 30% for the energy consumption evaluated by power (P), as well as the work developed by Andrade, et al. [29].

$$OBJ = \alpha M / M_{max} + \beta P / P_{max} \quad (3)$$

Considering that the forearm has a mass of 1.1 kg, the motor-reducer assembly has 0.231 kg, and it is necessary to allocate a portion of the mass to electronic components and batteries (0.5 kg), the maximum mass (M_{max}) allowed for the MR brake was 0.4 kg. The maximum power (P_{max}) adopted

was 14 W, equivalent to 20% of the engine power. As the objective is to present an actuator that better addresses user issues, mass reduction is a priority to provide better torque density, followed by power reduction to improve the energy consumption of the prosthesis.

The total mass of the MR brake is given by the sum of all parts of the system, as shown in Fig. 2, calculated by (4) where m_{coil} , m_{discs} , m_{MRF} , m_{core} and m_{al} represent the mass of the coil, the disks, the fluid, the core and aluminum (insulating layer and covering material), respectively.

$$M = m_{coil} + m_{discs} + m_{MRF} + m_{core} + m_{al} \quad (4)$$

The total power of the system is given by (5) as a function of current (I) and coil resistance, represented by the product of the coil average diameter (d_c), the electrical wire resistance per length (r_w), the number of turns in the coil (N_b) per π .

$$P = I^2 d_c r_w N_b \pi \quad (5)$$

Five design parameters were optimized: disks outer radius (r_0), core base radius (r_2), gaps numbers (N), fluid magnetic flux density (B_{MR}), and current (I). These parameters present restrictions, whose lower or upper limit values are obtained by trial and error during the optimization process [36]. The disks outer radius (r_0) was limited to 23 mm, considering that the wrist has a radius of 30 mm [7], with 2 mm for the cover thickness (L_3) and 5 mm for the prosthesis finishing. The radius of the core base (r_2) must be greater than the radius of the core inner (r_1) but less than the radius of the sum of the core inner radius with the side disks, since this thickness must have the same thickness as the core base, so there is no saturation. Therefore, the radius of the core base (r_2) must not exceed 8 mm. Due to manufacturing capacity, the number of gaps (N) was limited to 24.

The commercial fluid used is MRF 140-DG fluid from Lord Corporation. Depending on fluid properties, to reduce the non-linearity of the MR brake and facilitate fluid control, the maximum allowable MR flux density is 0.7 T [29]. As 25 AWG wire was used in coil manufacture, the maximum permissible current (I) is 2.5 A. The total mass (M) and the coil's power (P) must respect the conditions imposed on the objective function.

The lateral discs thickness (L_2) is restricted to the constructive character of the core. The shear limit stress and the relative magnetic permeability of the fluid must be considered for $B_{MR} < 0.7$ T so as not to saturate the system. The coils are designed in solenoid shape and multiple layers, allowing for a more compact form [29]. The core material is a low carbon steel (SAE 1020), a ferromagnetic material to increase magnetic flux density. This material presents magnetic saturation at 2.1 T. To avoid magnetic saturation in the brake core and disks, made of the same material, a magnetic flux density in the lower part of the core B_{core} (T) was limited to 2.0 T.

The coil's turns number N_b , which is restricted to the maximum cross-sectional area of the coil, can be written as in (6) [29]. In this case, it is considered that no circuit element has changed, L_5 is the insulation layer, L_1 is the width of the coil, and A_f represents the cross-sectional area of the coil wire.

$$N_b \leq [(r_i - L_5 - r_2)L_1]/A_f \quad (6)$$

Maximizing the resistive torque has a strong negative effect on the off-state torque and the weight of the brake [36]. It is because the ability of the handle to rotate freely when desired is essential [37]. Therefore, the off-state torque (T_{off}) was limited to 0.5 N.m not to impose restrictions on free movement. And the output torque (T) of an MR brake has the minimum value of 7.0 N.m required to meet activities of daily living, as mentioned above.

A short amputation (near the elbow) allows at least 108 mm for a wrist prosthesis [38]. The motor-reducer system is approximately 58 mm long. Therefore, the total width (L) of the brake MR must be a maximum of 25 mm to provide space for the other components of the prosthesis. For medium and long stump amputations, the pronation and supination movement can present a residual rotation of at least 100°, making the application of the MR brake less relevant [38].

Before any interaction of the PSO algorithm, the objective function was equal to 0.4280, with the mass and power equivalent to 0.1970 kg and 3.8837 W, respectively. After 150 interactions, the objective function converged, obtaining the minimum value of 0.3808. As a result, a mass of 0.1929 kg and a power of 2.0165 W were obtained. However, the number of gaps acquired is not an integer during the optimization process. The values of the optimized design variables are listed in Table I, and the number of gaps was rounding to the first upper interior. The results indicate that all the values obtained to meet the design constraints. The MR brake has a torque/mass ratio of 17.28 N.m/kg. The result is superior to the density of the human wrist, which is 7.27 N.m/kg, and the wrist with high torque density (8.38 N.m/kg) proposed in Chu, et al. [7]. The CAD drawing of the optimized prosthetic wrist is shown in Fig. 4.

C. Finite Element Analysis

The optimization results were verified using the finite element method (FEM), using ANSYS Mechanical APDL software. For this, the mesh with 0.15 mm was considered in a 2D configuration of the MR brake. The chosen relative permittivity was 1.0 for non-ferromagnetic materials. As input, the load was applied to the coil region. Finally, the magnetic flux was parallel to the outer edges as the MR brake elements were surrounded by air.

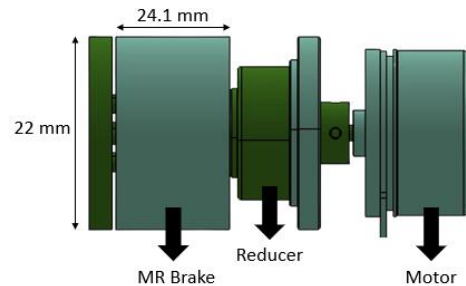


Figure 4. CAD model of the wrist prosthesis with the optimized dimensions of the MR brake. The light green color represents the structure connected to the stator and the dark green color represents the structure connected to the rotor.

TABLE I. OPTIMAL VALUE OF THE MR BRAKE VARIABLES

Project parameters	Restriction	Optimal value
Variables		
Disks outer radius (r_0)	23 mm (max)	20 mm
Core base radius (r_2)	8 mm (max)	7.5 mm
Gaps numbers (N)	24 gaps (max)	24 gaps
Fluid magnetic flux density (B_{MR})	0.7 T (max)	0.5645 T
Coil current (I)	2.5 A (max)	1.1138 A
Dependent variables		
Total mass (M)	0.4 kg (max)	0.1972 kg
Coil power (P)	14 W (max)	2.0821 W
Lateral disks thickness (L_2)	5.0 mm (max)	4.5 mm
Fluid maximum shear stress (τ_v)	$B_{MR} < 0.7$ T	34.225 kPa
Relative magnetic fluid permeability (μ_{MR})	$B_{MR} < 0.7$ T	$8.01 \cdot 10^{-6}$ T.m/A
Coil windings number (N_b)	$N_b \leq [(r_i - L_5 - r_2)L_1]/A_f$	$330 < 479$
Magnetic flux density at the core bottom (B_{core})	2.1 T (max)	1.9085 T
Torque in turn off-state (T_{off})	0.5 N.m (max)	0.0388 N.m
MR brake torque (T)	7.0 N.m (min)	7.4 N.m
Width (L)	25 mm (max)	24.1 mm

The results of the analysis via FEM are shown in Fig. 5. The magnetic flux density indicates that the magnetic field is perpendicular to the MR fluid region. This condition guarantees maximum shear strength, promoting better system functioning [29]. The maximum magnetic flux density is 1.8264 T. This value is similar to the value obtained in the optimization (1.9085 T), which confirms the developed equation. Furthermore, the FEM analysis shows that the variability of the magnetic flux density in the fluid region is low. Finally, there is no magnetic saturation in any part of the MR brake, and it works appropriately for the restrictions imposed.

The control and experimental validation of the project will be done in future works. Although the wrist has a satisfactory torque density, it is necessary to adjust the design to introduce other degrees of freedom, such as flexion and

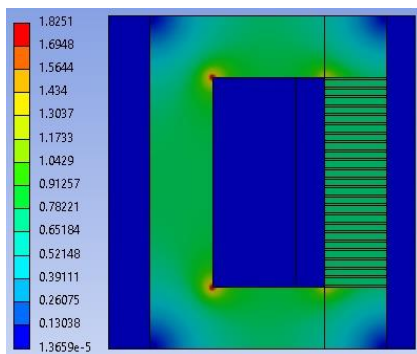


Figure 5. Magnetic finite element analysis of the optimized brake (currente 1.1138 A and values in T).

extension of the prosthesis.

IV. CONCLUSION

This work presented the design of an MR brake for the pronation and supination movement of a prosthetic wrist. The device is composed of a geared motor (EC 45 Flat motor and CSG-14-100-2A-RE Harmonic drive) responsible for the active torque, arranged in parallel with an MR brake, and is accountable for the resistive torque. With this configuration, the wrist actuator can replicate the kinetic characteristics of the human wrist in prono-supination movement. The dimensions of the MR brake were optimally designed with a PSO algorithm to minimize the mass and energy consumption of the system. The final design reached 0.1972 kg and 2.0821 W. The results indicate a great torque/volume and torque/mass ratio for prosthetic devices. In future work, we intend to manufacture a prototype for experimental validation and add the other degrees of freedom of the wrist.

REFERENCES

- [1] Y. Yoshii, H. Yuine, O. Kazuki, W.-L. Tung, and T. Ishii, "Measurement of wrist flexion and extension torques in different forearm positions," (in eng), *Biomed Eng Online*, vol. 14, pp. 115-115, 2015, doi: 10.1186/s12938-015-0110-9.
- [2] J. F. Kramer, D. Nusca, L. Bisbee, J. MacDemid, D. Kemp, and S. Boley, "Forearm Pronation and Supination: Reliability of Absolute Torques and Nondominant/Dominant Ratios," *Journal of Hand Therapy*, vol. 7, no. 1, pp. 15-20, 1994/01/01/ 1994, doi: [https://doi.org/10.1016/S0894-1130\(12\)80036-6](https://doi.org/10.1016/S0894-1130(12)80036-6).
- [3] Y. Lee, C. Chu, J. Xu, and C. Lan, "A Humanoid Robotic Wrist With Two-Dimensional Series Elastic Actuation for Accurate Force/Torque Interaction," *IEEE/ASME Transactions on Mechatronics*, vol. 21, no. 3, pp. 1315-1325, 2016, doi: 10.1109/TMECH.2016.2530746.
- [4] C. L. Semasinghe, D. G. K. Madusanka, R. K. P. S. Ranaweera, and R. A. R. C. Gopura, "Transradial prostheses: Trends in development of hardware and control systems," *The International Journal of Medical Robotics and Computer Assisted Surgery*, <https://doi.org/10.1002/rcs.1960> vol. 15, no. 1, p. e1960, 2019/02/01 2019, doi: <https://doi.org/10.1002/rcs.1960>.
- [5] J. E. Erickson, K. J. DeLaurentis, and M. Bouzit, "A Novel Single Digit Manipulator for Prosthetic Hand Applications," in *2007 IEEE Systems and Information Engineering Design Symposium*, 27-27 April 2007 2007, pp. 1-5, doi: 10.1109/SIEDS.2007.4373999.
- [6] N. M. Bajaj, A. J. Spiers, and A. M. Dollar, "State of the Art in Artificial Wrists: A Review of Prosthetic and Robotic Wrist Design," *IEEE Transactions on Robotics*, vol. 35, no. 1, pp. 261-277, 2019, doi: 10.1109/TRO.2018.2865890.
- [7] C. Chu, J. Xu, and C. Lan, "Development of a compact wrist mechanism with high torque density," in *2012 IEEE/ASME International Conference on Advanced Intelligent Mechatronics (AIM)*, 11-14 July 2012 2012, pp. 226-231, doi: 10.1109/AIM.2012.6265968.
- [8] M. Tavakolan and C. Menon, "Towards the development of a robust model for estimating wrist torque at different wrist angles," in *2012 IEEE International Conference on Robotics and Biomimetics (ROBIO)*, 11-14 Dec. 2012 2012, pp. 618-623, doi: 10.1109/ROBIO.2012.6491035.
- [9] K. H. Gudmundsson, F. Jonsdottir, and F. Thorsteinsson, "A geometrical optimization of a magneto-rheological rotary brake in a prosthetic knee," *Smart Materials and Structures (Print)*, vol. 19, no. 3, p. 11, 2010, doi: DOI:101088/0964-1726/19/3/035023.
- [10] R. Ahamed, S.-B. Choi, and M. M. Ferdous, "A state of art on magneto-rheological materials and their potential applications," *Journal of Intelligent Material Systems and Structures*, vol. 29,

- no. 10, pp. 2051-2095, 2018/06/01 2018, doi: 10.1177/1045389X18754350.
- [11] O. Arteaga, J. Escorza, I. Medina, R. Navas, K. Amores, and J. Morales, "Prototype of Robotic Ankle-Foot Prosthesis with Active Damping Using Magnetorheological Fluids," *International Journal of Mechanical Engineering and Robotics Research*, pp. 753-758, 01/01 2019, doi: 10.18178/ijmerr.8.5.753-758.
- [12] C. Li *et al.*, "Research and Development of the Intelligently-Controlled Prosthetic Ankle Joint," in *2006 International Conference on Mechatronics and Automation*, 25-28 June 2006 2006, pp. 1114-1119, doi: 10.1109/ICMA.2006.257781.
- [13] D. Hua, X. Liu, Z. Li, P. Fracz, A. Hnydiuk-Stefan, and Z. Li, "A Review on Structural Configurations of Magnetorheological Fluid Based Devices Reported in 2018-2020," *Frontiers in Materials*, 10.3389/fmats.2021.640102 vol. 8, p. 24, 2021. [Online]. Available: <https://www.frontiersin.org/article/10.3389/fmats.2021.640102>.
- [14] A. Ç. T. Orhanlı, A. Yılmaz, and Ş. İ., "Dynamic tests of MR (Magnetorheologic) damper and analysis of response characteristics in semi-active knee prosthesis," in *2017 25th Signal Processing and Communications Applications Conference (SIU)*, 15-18 May 2017 2017, pp. 1-4, doi: 10.1109/SIU.2017.7960405.
- [15] R. M. de Andrade, J. S. R. Martins, M. Pinotti, A. B. Filho, and C. B. S. Vimieiro, "Novel active magnetorheological knee prosthesis presents low energy consumption during ground walking," *Journal of Intelligent Material Systems and Structures*, p. 1045389X20983923, 2021, doi: 10.1177/1045389X20983923.
- [16] B.-K. Song, S.-R. Kang, S.-W. Cha, Y.-H. Hwang, J.-S. Oh, and S.-B. Choi, "Design of a novel 6-DOF haptic master mechanism using MR clutches and gravity compensator," *Mechanics Based Design of Structures and Machines*, vol. 46, no. 6, pp. 767-780, 2018/11/02 2018, doi: 10.1080/15397734.2018.1469094.
- [17] G. Han Gyeol, P. Jong Min, C. Seung-Bok, and S. Jung Woo, "Development of haptic system for surgical robot," in *Proc.SPIE*, 2017, vol. 10164, doi: 10.1117/12.2259826. [Online]. Available: <https://doi.org/10.1117/12.2259826>
- [18] N. Quoc Hung, N. Phuong Bac, and C. Seung-Bok, "Optimal design of a hybrid MR brake for haptic wrist application," in *Proc.SPIE*, 2011, vol. 7977, doi: 10.1117/12.880396. [Online]. Available: <https://doi.org/10.1117/12.880396>
- [19] M. Avraam, M. Horodincea, P. Letier, and A. Preumont, "Portable smart wrist rehabilitation device driven by rotational MR-fluid brake actuator for telemedicine applications," in *2008 IEEE/RSJ International Conference on Intelligent Robots and Systems*, 22-26 Sept. 2008 2008, pp. 1441-1446, doi: 10.1109/IROS.2008.4650887.
- [20] L. Pan, Z. Yang, and D. Zhang, "A structurally decoupled mechanism for measuring wrist torque in three degrees of freedom," *Review of Scientific Instruments*, vol. 86, no. 10, p. 104301, 2015/10/01 2015, doi: 10.1063/1.4932556.
- [21] B. F. Morrey, L. J. Askew, and E. Y. Chao, "A biomechanical study of normal functional elbow motion," *JBJS*, vol. 63, no. 6, 1981. [Online]. Available: https://journals.lww.com/jbjsjournal/Fulltext/1981/63060/A_bio_mechanical_study_of_normal_functional_elbow.2.aspx.
- [22] V. M. Ciriello, R. V. Maikala, and N. V. O'Brien, "Maximal Acceptable Torques of Highly Repetitive Screw Driving, Wrist Flexion and Extension with a Pinch grip, Ulnar Deviation, and Handgrip Tasks for Seven Hour Workdays for Male Industrial Workers," *Proceedings of the Human Factors and Ergonomics Society Annual Meeting*, vol. 55, no. 1, pp. 968-970, 2011/09/01 2011, doi: 10.1177/1071181311551201.
- [23] V. M. Ciriello, R. V. Maikala, and N. V. O'Brien, "Maximal Acceptable Torques of Six Highly Repetitive Hand-Wrist Motions for Male Industrial Workers," *Human Factors*, vol. 55, no. 2, pp. 309-322, 2013/04/01 2012, doi: 10.1177/0018720812454539.
- [24] M. Lorenz *et al.*, "Wrist at risk? – Considerations derived from a novel experimental setup to assess torques during hip reaming with potential implications on the orthopedic surgeons' health," *Journal of the Mechanical Behavior of Biomedical Materials*, vol. 113, p. 104160, 2021/01/01/ 2021, doi: <https://doi.org/10.1016/j.jmbbm.2020.104160>.
- [25] Z. Hussain and N. Z. Azlan, "3-D Dynamic Modeling and Validation of Human Arm for Torque Determination During Eating Activity Using Kane's Method," *Iranian Journal of Science and Technology, Transactions of Mechanical Engineering*, vol. 44, no. 3, pp. 661-694, 2020/09/01 2020, doi: 10.1007/s40997-019-00299-8.
- [26] M. Kaneko *et al.*, "A Measurement of A Motion of Pronation and Supination of A Forearm for Healthy Subjects using Wireless Acceleration and Angular Velocity Sensors," in *World Congress on Medical Physics and Biomedical Engineering May 26-31, 2012, Beijing, China*, Berlin, Heidelberg, M. Long, Ed., 2013// 2013: Springer Berlin Heidelberg, pp. 700-703.
- [27] A. M. Valevicius *et al.*, "Characterization of normative angular joint kinematics during two functional upper limb tasks," *Gait & Posture*, vol. 69, pp. 176-186, 2019/03/01/ 2019, doi: <https://doi.org/10.1016/j.gaitpost.2019.01.037>.
- [28] H. G. Gang, S.-B. Choi, and J. W. Sohn, "Experimental Performance Evaluation of a MR Brake-Based Haptic System for Teleoperation," *Frontiers in Materials*, 10.3389/fmats.2019.00025 vol. 6, p. 25, 2019. [Online]. Available: <https://www.frontiersin.org/article/10.3389/fmats.2019.00025>.
- [29] R. M. Andrade, A. B. Filho, C. B. S. Vimieiro, and M. Pinotti, "Optimal design and torque control of an active magnetorheological prosthetic knee," *Smart Materials and Structures*, vol. 27, no. 10, p. 105031, 2018/09/17 2018, doi: 10.1088/1361-665x/aadd5c.
- [30] Q.-H. Nguyen and S.-B. Choi, "Optimal Design Methodology of Magnetorheological Fluid Based Mechanisms," *Smart Actuation and Sensing Systems - Recent Advances and Future Challenges*, IntechOpen, Ed., 2012. [Online]. Available: <https://www.intechopen.com/chapters/39986>
- [31] H. Sayyaadi and S. H. Zareh, "Prosthetic knee using of hybrid concept of magnetorheological brake with a T-shaped drum," in *2015 IEEE International Conference on Mechatronics and Automation (ICMA)*, 2-5 Aug. 2015 2015, pp. 721-726, doi: 10.1109/ICMA.2015.7237574.
- [32] R. S. T. Saini, H. Kumar, S. Chandramohan, and S. Srinivasan, "Optimal Design of Rotary Magneto-Rheological Drum Brake for Transfemoral Prosthesis," in *Recent Advances in Computational Mechanics and Simulations*, Singapore, S. K. Saha and M. Mukherjee, Eds., 2021// 2021: Springer Singapore, pp. 465-474.
- [33] F. Gao, Y.-N. Liu, and W.-H. Liao, "Optimal design of a magnetorheological damper used in smart prosthetic knees," *Smart Materials and Structures*, vol. 26, no. 3, p. 035034, 2017/02/13 2017, doi: 10.1088/1361-665x/aa5494.
- [34] K. H. Gudmundsson, F. Jonsdottir, and F. Thorsteinsson, "A Multi-Objective Design Optimization of a Smart Magneto-Rheological Prosthetic Knee," 2009. [Online]. Available: <https://doi.org/10.1115/SMASIS2009-1237>.
- [35] R. M. Andrade, A. B. Filho, C. B. S. Vimieiro, and M. Pinotti, "Evaluating Energy Consumption of an Active Magnetorheological Knee Prosthesis," in *2019 19th International Conference on Advanced Robotics (ICAR)*, 2-6 Dec. 2019 2019, pp. 75-80, doi: 10.1109/ICAR46387.2019.8981642.
- [36] S. H. Mousavi and H. Sayyaadi, "Optimization and Testing of a New Prototype Hybrid MR Brake With Arc Form Surface as a Prosthetic Knee," *IEEE/ASME Transactions on Mechatronics*, vol. 23, no. 3, pp. 1204-1214, 2018, doi: 10.1109/TMECH.2018.2820065.
- [37] F. Jonsdottir, E. T. Thorarinnsson, H. Pálsson, and K. H. Gudmundsson, "Influence of Parameter Variations on the Braking Torque of a Magnetorheological Prosthetic Knee," *Journal of Intelligent Material Systems and Structures*, vol. 20, no. 6, pp. 659-667, 2009/04/01 2008, doi: 10.1177/1045389X08094303.
- [38] C. L. Taylor, "The biomechanics of control in upper-extremity prostheses," *Orthot Prosthet* vol. 35:20, 1981.